Journal of Quantitative Spectroscopy & Radiative Transfer 110 (2009) 1490–1501

Contents lists available at ScienceDirect

Journal of Quantitative Spectroscopy & Radiative Transfer

journal homepage: www.elsevier.com/locate/jqsrt

Size characteristics of surface plasmons and their manifestation in scattering properties of metal particles

K. Kolwas *, A. Derkachova, M. Shopa

Institute of Physics, Polish Academy of Sciences, Al. Lotników 32/46, Warszawa, Poland

ARTICLE INFO

Article history:
Received 24 November 2008
Received in revised form
25 February 2009
Accepted 17 March 2009

Keywords:
Multipolar surface plasmon oscillations
Plasmon size dependent properties
Surface plasmon resonance
Silver nanoparticles
Gold nanoparticles
Electromagnetic field enhancement
Sensing
Scattering properties of metallic particles
Mie theory

ABSTRACT

The change of the scattering properties of sodium, gold and silver spherical particles with size is discussed in the context of surface multipolar plasmon resonances. The presented surface plasmon size characteristics are abstracted from the quantity which is observed and deliver multipolar plasmon resonance frequencies and plasmon damping rates in the form of a continuous function of particle radius. The performed analysis of the plasmon dispersion relation is analogous to the problem of surface plasmon localized at a semi-infinite, flat metal/dielectric interface.

Correlation between the multipolar plasmon resonance parameters, and the spectroscopic optical properties of conductive nanoparticles appearing as peaks in the measurable light intensities is analyzed. We discuss the fact, that such peaks arise from interference of all the electromagnetic fields contributing to the measured intensity, and not solely to the fields due to surface plasmon multipolar modes.

We describe the results of light scattering experiment in orthogonal polarization geometries with use of spontaneously growing sodium droplets. The polarization geometry of the experiment allows for distinct separation of resonant contribution of dipole and quadrupole plasmon TM mode contributions to the measured intensities as a function of size.

Predictions concerning size characteristics for dipole and quadrupole plasmons are compared with the results of light scattering experiments using spherical sodium droplets (our results) and gold and silver particles in suspension [other authors: Sönnichsen C, Franzl T, Wilk T, von Plessen G, Feldmann J. Plasmon resonances in large noble-metal clusters. New J Phys 2002; 4:93.1–8; Haiss W, Thanh NTK, Aveyard J, Fernig DG. Determination of size and concentration of gold nanoparticles from UV–vis spectra. Anal Chem 2007; 79:4215–21; Njoki PN, Lim I-IS, Mott D, Park H-Y, Khan B, Mishra S, et al. Size correlation of optical and spectroscopic properties for gold nanoparticles. J Phys Chem C 2007; 111:14664–9; Mock JJ, Barbic M, Smith DR, Schultz DA, Schultz S. Shape effects in plasmon resonance of individual colloidal silver nanoparticles. J Chem Phys 2002; 116:6755–9].

* Corresponding author.
E-mail addresses: Krystyna.Kolwas@ifpan.edu.pl (K. Kolwas), Anastasiya.Derkachova@ifpan.edu.pl (A. Derkachova), shopa@ifpan.edu.pl (M. Shopa).

0022-4073/$ - see front matter © 2009 Elsevier Ltd. All rights reserved.
doi:10.1016/j.jqsrt.2009.03.020

1. Introduction

Surface plasmon (SP) excitations are known to contribute to exceptional optical properties of metal nanostructures. Excitation of SP oscillations with light at metal–dielectric interface is a fascinating phenomenon of great potential application in nanophotonics, biophotonics, sensing, biochemistry and medicine [5].

Excitation of surface plasmons at optical frequencies, guiding them along the interface, and coupling them back into freely propagating light are processes of great interest for the manipulation and transmission of light at the nanoscale. The example can be nondiffraction-limited guiding of light fields via a linear chain of gold nanoparticles: spheres [6–9] and nanowires [10]. Metallic nanostructures can serve as potential building blocks for the fabrication of materials with negative refractive index (metamaterials).

An important application of localization and thus enhancement of the near electromagnetic fields due to plasmon excitations is surface enhanced Raman spectroscopic (SERS) technique [11,12]. It allows detection of trace amount of molecules, microorganisms or living cells adsorbed at the surface of metallic nanostructure illuminated with light at a wavelength corresponding to the plasmon resonance frequency. Applications of SERS in biology, biochemistry and biomedicine are of great importance. Examples can be the spectroscopy of single bacteria of *Escherichia coli* [13] or of neurotransmitters [14]. Plasmons excited in metal nanoshells bound to tumor proteins are tested in photothermal tumor therapy. The large effective scattering cross-section of individual noble metal nanoparticles at plasmon resonance condition, as well as their nonbleaching properties have significant potential for single molecule labeling based biological assays [15–17].

Thus, there is a substantial and broad interest in the fundamental properties of SP propagation in nanoscale structured matter. Intrinsic properties of SP are determined by the respective dispersion relations. In contrast to bulk metal with a flat surface, the excitation of collective motion of free electrons at the surface of a metallic nanoparticle of a curved surface is possible by direct optical means. Metallic structures smaller than the wavelength of incident light demonstrate fascinating optical properties which are highly dependent on the particle material, size and shape. In contrast to the dispersion relation for an SP at a planar metal/dielectric interface, which is well-investigated theoretically and experimentally, [18–20], the dispersion relation at a curved surface is much less explored [20,21]. Such relation is important from a fundamental perspective but may also provide exciting ways of exploiting the optical properties of nanoparticles.

Recent progress in synthesis and functionalization of noble metal nanoparticles (e.g. spherical gold and silver standardized nanospheres of well-defined radii are available commercially) and nanorods [22–24] caused a rapid growth in the number of studies of surface plasmon properties in free (or colloidal), and supported nanostructures. The assignment and interpretation of multipole resonances in nanorods have been usually done indirectly, on the basis of the standing wave picture [25,26] and DDA calculations [27]. However, the DDA algorithm does not include an explicit multipole representation. Therefore, there are only limited data on the multipole plasmon resonances in nanorods [27,28], and nanoprisms [29]. Surprisingly, the same applies to nanospheres [1–3].

In many applications, the size characteristics of multipolar surface plasmons are crucial. The spherical nanoparticle is geometrically the simplest nanostructure of single parameter defining the size. A spherical symmetry of the nanostructure enables rigorous description of plasmon features within the framework of classical electrodynamics. That allows, in principle, relatively simple analysis of the dispersion relation of surface plasmons and their size dependent multipolar features. In spite of this geometrical simplicity, there are few direct data reporting size dependence of plasmon characteristics resulting from the dispersion relation for particles of various metals [30–33].

Our modeling of plasmon size characteristics is based on surface plasmon dispersion relations. This allows the description of plasmons as an intrinsic property of a metal nanosphere embedded in a dielectric medium, which does not depend on the measured quantity. That property allows for resonant excitation of collective oscillations of free electrons at the interface. When excited, a metal sphere acts as radiating antenna at characteristic radius dependent frequencies. In order to find plasmon size characteristics we look for the eigenmodes of self-consistent, divergence free Maxwell equations fulfilling continuity relations at the sphere boundary. Conditions for existence of transverse magnetic solutions (with the nonzero normal to the interface component of the electric field) define complex eigenfrequencies of the fields Ω_l with $l = 1, 2, 3, \ldots$. $Re(\Omega_l) = \omega'_l(R)$ define the frequencies of the field, which can couple to collective electron oscillations (plasmons) in a sphere of radius R. The discussion is concentrated on size characteristics of the plasmon oscillation frequencies and their manifestations in some quantities, that can be measured in far and near field. The size-dependent damping rates $Im(\Omega_l) = \omega''_l(R)$ [30,31] are not discussed in this paper.

The notion of plasmons is connected with transverse magnetic surface electromagnetic fields, while light intensities (irradiance), that can be measured, are inevitably composed of both TM and TE components of different polarity l. Both contributions interfere forming a complex pattern depending on the geometry of observation and on the size of a particle in comparison with the wavelength of the light being scattered. The result of the negative interference can result in cancellation or smearing out of plasmon electromagnetic field contribution to the intensity of light scattered in a given direction. It is why the maxima in quantities such as the back scattering cross-section or a total extinction cross-sections, calculated on the base of Mie scattering theory, can differ from the plasmon resonance position, as derived from the dispersion relation for the plasmon electromagnetic fields.

Our analysis of plasmon size characteristics concerns sodium (the best free-electron metal used as a elementary check of a model), gold and silver (noble metal) spherical particles up to a particle size of about 300 nm in diameter. Noble metal nanoparticles have great potential application. They can serve as building blocks for optoelectronic devices, for guiding light, data storage, ultra-fast switching, sensors, etc. In gold and silver nanoparticles, plasmons can be excited at frequencies that can be tuned through the visible range. Knowing size characteristics of dipole and higher polarity plasmon resonance frequencies and plasmon damping rates, it is possible to tailor plasmon features according to the application in mind by choosing the appropriate size and material of the nanosphere and also the environment it resides in. Our study results in the ready-to-use, continuous functions of particle radius, which can be used to plan parameters of plasmon resonances in practical applications by choosing the appropriate size of the particle in the optically known dielectric environment. Our results could be especially useful for example in SERS spectroscopic technique, where data concerning the enhancement of electric field intensity (and not the radiation intensity) are of importance.

Our predictions concerning plasmon resonance frequencies are compared with several experimental observations. This comparison includes our experimental results for free sodium particles, where we studied the smooth change of their sizes with time up to a macroscopic droplet of the order of the wavelength of light. Our expectations concerning plasmon resonance frequencies in gold and silver nanoparticles are compared with the results obtained from the light scattering spectra reported in [1–3].

2. Mie scattering theory and the eigenvalue problem for the sphere

Since the first systematic study of Faraday [34], it is known, that even the merest or slight variation in the size of (gold) particles gives rise to a variety of colors of colloidal particles. As shown by Mie [35], elastic scattering of light and not absorption, is the process defining the spectacular color effects observed in suspensions of spherical metal (originally gold) particles with radii above tenths of nanometers. The contemporary illustration can be the image from dark-field microscope representing the result of scattering of white light by 30 nm silver nanoparticles and by clusters of nanoparticles of different sizes (see [36]).

Mie scattering theory allows describing the scattering of a plane monochromatic wave by a homogeneous sphere surrounded by a homogeneous medium for any particle radius and of any material. It deals with the problem of the continuity of the tangent component of the total electromagnetic fields fulfilling Maxwell's equations outside and inside the sphere. The fields outside the sphere include the incident field of the plane light wave arriving from a distinct source not included in Maxwell equations. The problem is solved in spherical coordinates, where electromagnetic fields are expressed as infinite sums of the partial electromagnetic waves of the "electric" (or transverse magnetic, TM) and "magnetic" (or transverse electric, TE) type, that are reciprocally orthogonal [37–40]. However, Mie scattering theory does not deal with the problem of surface electron density oscillations (surface plasmons) coupled to surface localized electromagnetic fields, although usually positions of successive peaks appearing in light scattering spectra of conducting particles obtained with Mie theory, are interpreted as directly related to positions of surface plasmon resonances.

In the description we use, spectrally selective optical effects in scattering properties of metal nanoparticles are not due to elastic scattering of the incident light nor to absorption, but rather to the elementary, intrinsic property of a conducting spherical nanostructure embedded in a dielectric medium that can manifest in the optical response to the external electromagnetic field. A conducting sphere is treated as an radiating antenna (a resonant circuit), that can be can be characterized by some discrete, resonance frequencies $\omega_l'(R)$, defined by a particle radius R for given metal and given sphere environment. The problem we consider is formulated in the absence of external, incoming fields and external charge sources, in analogy to the description of surface plasmons at a flat metal–dielectric interface [20,21], with the dispersion relation of the electromagnetic wave at the metal–dielectric interface treated as a central problem. The problem is solvable only for complex frequencies of the dispersion relation, that are size dependent. That makes an important difference in comparison with Mie theory, where the real frequency of the electromagnetic fields is an external, independent parameter of the theory.

Collective surface charge density oscillations (surface plasmons) at a spherical interface can only be due to the electromagnetic waves with a nonzero normal to the surface component of the electric field, so to the TM mode only, with the nonzero radial component of the electric field [20,21,39,40]. At that point there exist a correspondence between plasmons at spherical interface and surface plasmons that can propagate along a semi-infinite plane of a metal–dielectric flat interface [20,41]. It is well known, that such surface plasmons can be coupled to the p polarized electromagnetic wave only. For historical reasons, the orthogonal polarizations p (TM) and s (TE) of the incident wave were defined according to the direction of the electric (magnetic) field of the wave with respect to the plane of incidence. However, when considering possibility of surface charge density oscillations, the presence or absence of the normal to the surface component of the electric field is essential. The p (TM) polarized wave does contain the nonzero normal to the interface component of the electric field. Irrespective of the shape of the interface, conservation of the normal component of the electric displacement (so the continuity of $D_r(r=R,\omega)$ at a spherical metal–dielectric interface) is assured, if a jump in normal to the surface component of the electric field $E_\perp$ (which equals E_r for a spherical interface) is compensated by a polarization charge at a interface that oscillates at the electromagnetic field frequency. For a metal–dielectric boundary discussed here, surface polarization charge is due to collective motion of metal free electrons at a boundary. TE (or s polarized) fields cannot be

coupled to any surface charge oscillations. We note that Mie theory always deals with the incident field of both transverse magnetic (or "electric") and transverse electric (or "magnetic") waves: there is no polarization geometry, that allows the separation of these two waves and to use only one as an incident field. That introduces an important difference in scattering from spherical (Mie theory) and from a flat interface (Fresnel equations), while in this last case it is possible to separate p polarization from s polarization geometry.

Formally, the surface plasmon dispersion relation for electromagnetic waves at a spherical interface corresponds to the zeros of the complex denominators of one of the so-called Mie coefficients b_l (or ${}^{TM}B_l$), which together with a_l (or ${}^{TM}B_l$) Mie coefficient define the extinction and scattering cross-sections through the well-known relations [37–40]:

$$\sigma_{ext} = \frac{\lambda^2}{2\pi}\sum_{l=1}^{\infty}(2l+1)Re({}^{TM}B_l + {}^{TE}B_l), \tag{1}$$

$$\sigma_{sca} = \frac{\lambda^2}{2\pi}\sum_{l=1}^{\infty}(2l+1)[|{}^{TM}B_l|^2 + |{}^{TE}B_l|^2], \tag{2}$$

$$\sigma_{abs} = \sigma_{ext} - \sigma_{sca}, \tag{3}$$

where

$${}^{TM}B_l = \frac{\sqrt{\varepsilon_{in}}\psi_l'(\rho\sqrt{\varepsilon_{out}})\psi_l(\rho\sqrt{\varepsilon_{in}}) - \sqrt{\varepsilon_{out}}\psi_l(\rho\sqrt{\varepsilon_{out}})\psi_l'(\rho\sqrt{\varepsilon_{in}})}{\sqrt{\varepsilon_{in}}\xi_l'(\rho\sqrt{\varepsilon_{out}})\psi(\rho\sqrt{\varepsilon_{in}}) - \sqrt{\varepsilon_{out}}\xi_l(\rho\sqrt{\varepsilon_{out}})\psi_l'(\rho\sqrt{\varepsilon_{in}})}, \tag{4}$$

$${}^{TE}B_l = \frac{\sqrt{\varepsilon_{in}}\psi_l(\rho\sqrt{\varepsilon_{out}})\psi_l'(\rho\sqrt{\varepsilon_{in}}) - \sqrt{\varepsilon_{out}}\psi_l'(\rho\sqrt{\varepsilon_{out}})\psi_l(\rho\sqrt{\varepsilon_{in}})}{\sqrt{\varepsilon_{in}}\xi_l(\rho\sqrt{\varepsilon_{out}})\psi_l'(\rho\sqrt{\varepsilon_{in}}) - \sqrt{\varepsilon_{out}}\xi_l'(\rho\sqrt{\varepsilon_{out}})\psi_l(\rho\sqrt{\varepsilon_{in}})}. \tag{5}$$

It is often believed, that the resonances in the above crosses (4) and (5) may be directly associated with the corresponding resonances of the Mie coefficients (4) and (5), resulting from their denominators approaching 0. However, these denominators, which are composed of complex functions of complex arguments and derivatives of such functions with respect to the arguments, never can reach 0 for real ω's [30–32] of the incoming light wave. Therefore, in Mie scattering theory, where a frequency of the field is directly related to the incident light of wavelength λ, and is a real parameter, the real nor the imaginary part of the denominator of ${}^{m}B^{l}$ can never be equal to 0. All the measured quantities such as extinction and scattering cross-sections or the intensity of the light scattered in given direction, are composed not only from the sum of the TM and TE intensities (irradiances), but also from the interference of these contributions. However, only TM component can carry the contribution arising from a radiation emitted by the collective surface charge density oscillations that can be excited, if the frequency ω of the incident field fits to the plasmon resonance frequency $\omega_l'(R)$ in a sphere of radius R: $\omega = \omega_l'(R)$. Therefore, neither dipole plasmon in larger particles nor higher multipolarity plasmons have to correspond exactly to the maxima of the back or forward scattering cross-sections nor of total extinction cross-section; these quantities possess some maxima which are shifted with respect to each other.

2.1. Dielectric function and the dispersion relation

The indices of refraction $n(\omega) = \sqrt{\varepsilon(\omega)}$ of both media are input parameters of Mie theory and of the dispersion relation (11), which we consider. For metal particles in vacuum and being much smaller than the wavelength of the incident light (quasistatic approximation), Mie theory predicts the well-known resonance in the total absorption cross-section (the "giant Mie resonance" (e.g. [39,42,43])) at a frequency:

$$\omega_{Mie} = \frac{\omega_p}{\sqrt{3}} \tag{6}$$

assuming the similar dielectric function for the bulk ideal free-electron metal (the Drude dielectric function) and for a metal nanoparticle:

$$\varepsilon_m(\omega) = 1 - \frac{\omega_p^2}{\omega^2 + i\omega\gamma} \tag{7}$$

after neglecting the electron relaxation rate γ. ω_p is the plasma frequency of the bulk metal, defining its conduction-electron concentration. The same form of the Drude dielectric function has been used in the dispersion relation for a surface plasmon at a planar metal–dielectric interface (e.g. [18,19,44,20]):

$$k_{sp} = \frac{\omega}{c}\sqrt{\frac{\varepsilon_m(\omega)\varepsilon_d(\omega)}{\varepsilon_m(\omega) + \varepsilon_d(\omega)}}, \tag{8}$$

where k_{sp} is the wave vector of surface plasmon wave at a planar metal–dielectric interface, ε_d is a dielectric function of the material over the metal. For $\varepsilon_d = 1$, and $\varepsilon_m(\omega)$ with $\gamma = 0$, the surface plasmon flat-interface resonance

frequency is given by

$$\omega_{SP} = \frac{\omega_p}{\sqrt{2}}. \tag{9}$$

The Drude dielectric function is the simplest form of the analytic function describing the wavelength dependence of optical properties of free-electron metals, that can be used in modeling the metal optical properties. However, in practice it can be used only for the optical properties of sodium, with parameters $\omega_p = \sqrt{Ne^2/\varepsilon_0 m^*}$, where N and m^* is the density and the effective mass of the conduction electrons, respectively. In other alkali metals, as well as in noble metals, the interband transitions constitute important contribution to the optical properties. In addition, in small nanoparticles with radii R smaller than the electron mean free path in bulk metals, $R<l_\infty$, the frequency of electron collisions γ is modified by the presence of an interface and depends on the particle radius R [45].

In our modeling we account for the interband transitions in gold and silver nanoparticles by introducing the effective dielectric function:

$$\varepsilon_m(\omega) = \varepsilon_\infty - \frac{\omega_p^2}{\omega^2 + i\omega\gamma} \tag{10}$$

with the effective parameters $\varepsilon_\infty = 9.84$, $\omega_p = 9.096$ eV, $\gamma = 0.072$ eV for gold, and $\varepsilon_\infty = 3.7$ eV, $\omega_p = 8.9$ eV, $\gamma = 0.021$ eV for silver chosen in a way, that $n_{in} = \sqrt{\varepsilon_{in}(\omega)}$ reproduces reasonably well the measured real and imaginary parts of the refraction coefficients n [46] for these elements in the frequency ranges: 0.8–5.0 eV for gold and 0.8–4.2(4.0) eV for silver, with the parameter ε_∞ accounting for contribution of the interband transitions in those metals.

The optical properties of the dielectric medium outside the spheres are described by $\varepsilon_{out} = n_{out}^2$ and are assumed to be frequency independent, with n_{out} chosen as 1 or 1.5 in the calculations.

2.2. Electromagnetic eigenmodes for the metal sphere (plasmons)

The system considered is a homogeneous, nonmagnetic metal sphere of optical properties described by the frequency dependent dielectric function $\varepsilon_{in}(\omega)$ of known analytic form (Eq. (10)), and its surrounding dielectric of properties described by ε_{out}. The study is made in the light field wavelength range, where $Re\varepsilon_{in}(\omega) \leqslant 0$. We look for the eigenmodes of self-consistent, divergence free Maxwell equations that can be excited at the metal–dielectric interface. We follow the concept of [21], adopted in the book [20] dedicated to review of dispersion relations problems in solids and plasmas. We consider continuity relations at the spherical boundary for the tangent component of the transverse magnetic solution to the Helmholtz equation in spherical coordinates (e.g. [30,31]), while only TM solutions possess nonzero normal to the surface component of the electric field (see Section 2). Conditions assuring continuity of tangent components at a sphere boundary define the dispersion relation [30,31]:

$$\sqrt{\varepsilon_{in}(\omega)}\xi_l'(k_{out}(\omega)R)\psi_l(k_{in}(\omega)R) + \sqrt{\varepsilon_{out}(\omega)}\xi_l(k_{out}(\omega)R)\psi_l'(k_{in}(\omega)R) = 0, \tag{11}$$

which is fulfilled for the complex eigenfrequencies of the fields Ω_l, $l = 1, 2, 3, \ldots$ at $r = R$. $\psi_l(z)$ and $\xi_l(z)$ are Riccati–Bessel spherical functions, the prime marker ($'$) indicates differentiation with respect to the argument, $k_{in} = \omega/c\sqrt{\varepsilon_{in}(\omega)}$ and $k_{out} = \omega/c\sqrt{\varepsilon_{out}}$.

We solve Eq. (11) numerically with respect to complex values of $\Omega_l(R) = \omega_l'(R) + i\omega_l''(R)$ with the sphere radius R treated as an outside, independent parameter [30,31]. The real part of the radius dependent eigenvalues $\Omega_l(R)$ defines the surface plasmon oscillation frequencies $\omega_l'(R)$ for a mode l and the imaginary part $\omega_l''(R)$ defines the damping rates (reciprocal of damping times) of the surface free-electron oscillations in that mode, if excited. The solution to the problem is possible only for complex frequencies of the dispersion relation; plasmon oscillations are always damped (losses due to radiation and heat). It must be stressed that the solutions to the dispersion relation (11) exist only if $\omega_l''(R) \neq 0$. Plasmon oscillations at spherical boundary are always damped (at least) due to radiation of oscillating charge of surface free-electron densities waves (plasmons).

First, let us consider sodium as the best free-electron metal of optical properties well described by the analytic Drude free-electron dielectric function (7), and $\varepsilon_{out} = 1$ [30]. As shown in Fig. 1, the frequency of the dipole plasmon, as well as frequencies of plasmons of higher polarity, decreases with growing particle size. The dipole eigenmode at frequency just known from the quasistatic approximation: $\omega_{l=1}'(R_{\min,l=1}) = \omega_p\sqrt{3}$ can be attributed to a sphere starting from the smallest size limit.

Resonance takes place, when a frequency of the incoming light wave ω approaches the real part of the eigenfrequency of a sphere of given radius: $\omega = \omega_l'(R_l)$. The resonance condition is fulfilled for a well-defined size in each excited plasmon mode l: $R = R_{l=1,2\ldots}$, starting from the minimal value $R_{\min,l}$ characteristic for given polarity l. The same applies to the damping rates, which equals $|\omega_l''(R_{\min,l})| = \gamma/2$ for the characteristic minimal radii $R_{\min,l}$ in each multipolar mode l [31]. The corresponding frequencies of plasmons $\omega_l'(R_{\min,l})$ coincide with the values just known from the quasistatic approximation in the limit of vanishing size (e.g. [20,39,44]):

$$\omega_l'(R_{\min,l}) = \omega_p\sqrt{\frac{l}{2l+1}}. \tag{12}$$

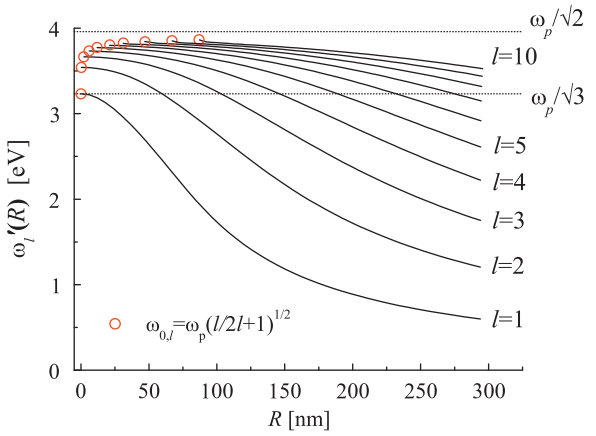

Fig. 1. Multipolar plasmon resonance frequencies $\omega_l'(R)$ as a function of radius R (rigorous modeling) for sodium nanospheres in vacuum ($n_{out} = 1$; solid lines).

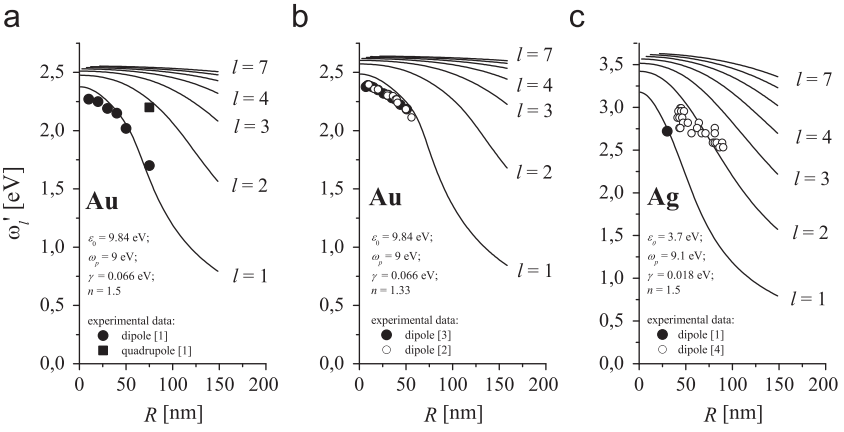

Fig. 2. (a) and (b) Multipolar ($l = 1, 2, \ldots, 7$) plasmon resonance frequencies as a function of sphere radius in a suspensions of index of refraction: $n_{out} = 1.5$ and 1.33 correspondingly for gold nanoparticles and (c) for silver nanoparticles in a suspension of $n_{out} = 1.5$. Open and black circles correspond to the experimental data on dipole plasmon position, a square corresponds to quadrupole plasmon position [1–4].

For $l = 1$, $\omega'_{l=1}(R_{\min,l=1})$ equals the well-known value of the Mie resonance frequency: $\omega_l'(R_{\min,l}) = \omega_{Mie}$ (Eq. (6)), as illustrated in Fig. 1. In the limit of large minimal radii $R_{\min,l}$ (and large l) one gets the value of the oscillation frequency of a plasmon at flat interface: $\omega_l'(R_{\min,l}) \to \omega_{sp}$ (Eq. (9)). The same features characterize gold and silver spheres in vacuum (in air), but the experiments with unsupported gold and silver nanospheres are usually performed in suspensions of particles.

Fig. 2 (solid lines) illustrates the obtained size dependence of multipolar ($l = 1, 2, \ldots 7$) plasmon oscillation frequencies of gold and silver nanoparticles embedded in environment of the refractive index $n = 1.5$. Contrary to some expectations, not only the dipole plasmon, but also higher polarity plasmon resonance frequencies can be attributed to particles of size as small as 10 nm. With growing size, the individual resonances are spectrally better resolved.

2.3. *Manifestation of plasmon excitations in light scattered in orthogonal polarization geometries (Mie scattering theory)*

Positions of maxima in the intensity of light scattered or transmitted by particles can deliver an indirect, sometimes approximated information about multipolar plasmon resonance position in particles with radii above some tenths of nanometers.

Let us consider at first the scattering properties of sodium nanospheres, in the directions orthogonal to the direction of the incident light beam: parallel and perpendicular to the direction of the incoming light field polarization (see Fig. 3).

According to the results of Mie scattering theory, the dependence of the intensities of light of frequency ω elastically scattered in directions orthogonal to the direction of the incident light beam on the particle size is described as

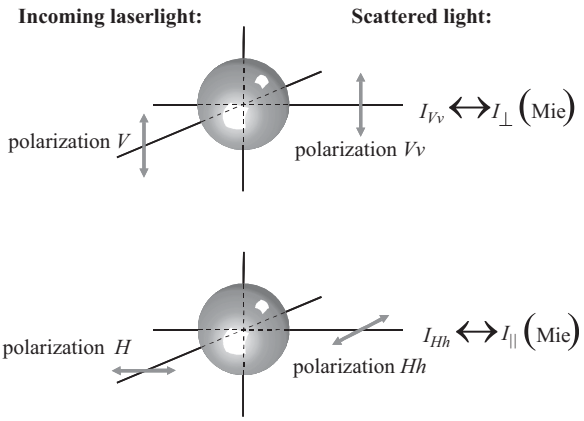

Fig. 3. Scheme of polarization geometry.

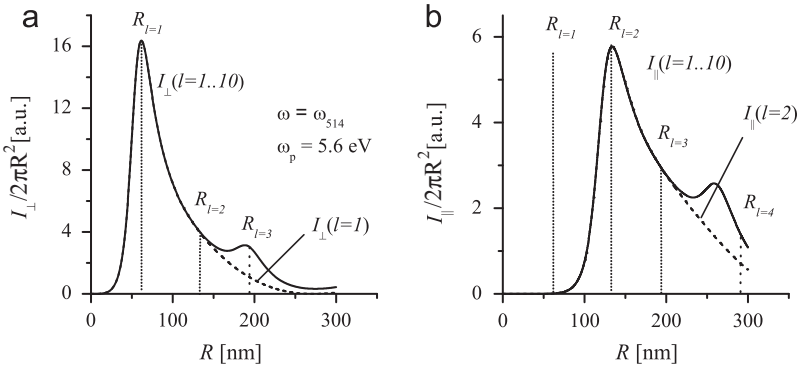

Fig. 4. The dependency of the $I_{\perp}(R)/2\pi R^2$ and $I_{\parallel}(R)//2\pi R^2$ intensities scattered in orthogonal polarization geometries (Fig. 3) by a sodium sphere calculated from Mie theory (solid line) for the incoming light of wavelength $\lambda = 514\,\text{nm}$ ($\omega_{514} = 2.41\,\text{eV}$). Dashed line represents the contribution of the TM mode only to the intensities, with single $l = 1$ (a) and $l = 2$ (b) contributions. Horizontal dotted line represent radii R_l allowing to fulfill the resonance condition $\omega_{514} = \omega_l(R_l)$ as expected from solving the plasmon eigenmodes problem (see Fig. 1).

follows [38]:

$$I_{\perp}(R) = \frac{1}{\pi R^2}\left[\frac{\lambda}{2\pi r}\left|\sum_{l=1}^{\infty} i\frac{2l+1}{l(l+1)}\left({}^{TM}B_l(R)P_l^{(1)'}(\cos\Theta)\sin\Theta - {}^{TE}B_l(R)\frac{P_l^{(1)}(\cos\Theta)}{\sin\Theta}\right)\right|\right]^2, \tag{13}$$

$$I_{||}(R) = \frac{1}{\pi R^2}\left[\frac{\lambda}{2\pi r}\left|\sum_{l=1}^{\infty} i\frac{2l+1}{l(l+1)}\left({}^{TM}B_l(R)\frac{P_l^{(1)}(\cos\Theta)}{\sin\Theta} - {}^{TE}B_l(R)P_l^{(1)'}(\cos\Theta)\sin\Theta\right)\right|\right]^2. \tag{14}$$

We concentrate on the role of the TM mode of the electromagnetic field in these quantities, as only this mode can carry information about surface plasmon resonance manifestation to the intensities $I_{\perp}(R)$ and $I_{\parallel}(R)$, (13) and (14), as discussed in the previous sections.

Our results show that the size dependence of multipolar plasmon resonance frequencies in sodium spheres (Fig. 1), for light of $\omega_{514} = 2.412\,\text{eV}$, the dipole plasmon resonance $\omega_{514} = \omega'_{l=1}(R_{l=1})$ is expected for a sphere of radius R approaching the value $R_{l=1} = 62\,\text{nm}$, and the quadrupole plasmon resonance $\omega_{514} = \omega'_{l=2}(R_{l=2})$ is expected for $R_{l=2} = 129\,\text{nm}$.

The maxima in the size dependence of the intensities per unit surface $I_{\perp}(R)/2\pi R^2$ and $I_{\parallel}(R)//2\pi R^2$ resulting from the Mie theory coincide with these expectations (see Fig. 4). Both TM and TE components of the electromagnetic fields contribute to the scattering intensities $I_{\perp}(R)$ and $I_{\parallel}(R)$, (13) and (14). However, due to the particular geometry of observation, conditions for observing contribution of secondary fields re-emitted by plasmons with successive values $l = 1$ and 2 are not the same in every direction. Let us consider the example presented in Fig. 4, where solid lines represent the intensities per unit surface $I_{\perp}(R)/2\pi R^2$ and $I_{\parallel}(R)//2\pi R^2$ of light at wavelength $\lambda = 514\,\text{nm}$, scattered in orthogonal geometries (Fig. 4(a) and (b) correspondingly), while dashed line represents the contribution of only TM modes of the field to these quantities. In the particle size range up to $R = 150\,\text{nm}$, the TM dipole ($l = 1$) mode contribution dominates in the total scattered light

intensity $I_{\perp}(R)/2\pi R^2$ (Fig. 4(a)), while the TM quadrupole ($l=2$) mode dominates in $I_{\parallel}(R)//2\pi R^2$ intensity (Fig. 4(b)). $l=1$ contribution is absent, while the dipole plasmonic antenna does not radiate in this direction.

This analysis leads to the conclusion, that the position of maximum in $I_{\perp}(R)/2\pi R^2$ and in $I_{\parallel}(R)//2\pi R^2$ for chosen values of ω of the incident light can be attributed to excited plasmon resonance contribution correspondingly: dipole and quadrupole one. TE mode contribution is negligible. This result allows us to conclude, that the maxima in $I_{Vv}(R)/2\pi R^2$ and $I_{Hh}(R)/2\pi R^2$ resulting from our light scattering experiment on sodium light induced droplets (see Fig. 3 and Section 3.1), are real manifestation of plasmon resonances, and not a kind of artefact resulting from the complex interference pattern of the TM and TE mode contributions of different multipolarity.

The observation in orthogonal polarization geometry is the unique experimental scheme allowing the direct separation of the pure dipole and quadrupole plasmon resonances. This is not possible with any other type of observation and will be discussed further in Section 2.4.

2.4. Manifestation of plasmon excitations in spectra in a particle of given size (Mie scattering theory)

Let us consider now some scattering spectra of a suspension ($n_{out}=1,5$) of gold particles of chosen radius as an illustration of problems one can encounter when trying to find size dependence of multipolar plasmon resonances.

According to our results concerning plasmon positions in such spheres (Figs. 2(a) and 5(a), dotted vertical lines), several multipolar plasmons of different l could contribute to the scattered light spectrum for clusters as small as $R=10$ nm. For that size, multipolar contributions are concentrated in a relatively narrow spectral range. For nanospheres as small as 10 nm, only one peak in the total scattering cross-sections can be observed at an eigenfrequency corresponding to the dipole plasmon resonance $\omega'_{l=1}=2.38$ eV, in spite the resonance condition is fulfilled for some higher multipolar frequencies as well (see Fig. 2).

For a nanosphere with a radius of 60 nm, the dipole plasmon resonance eigenfrequency $\omega'_{l=1}(R=60\,\text{nm})=1.93$ eV does still coincides with the strongly broadened maxima in the scattering cross-sections (see Figs. 2(a) and 5(b), dotted vertical lines). However, the quadrupole plasmon resonance frequency $\omega'_{l=2}(R=60\,\text{nm})=2.37$ eV and higher polarity plasmon resonance frequencies do not coincide obligatory with the positions of maxima in the back-scattering cross-sections nor

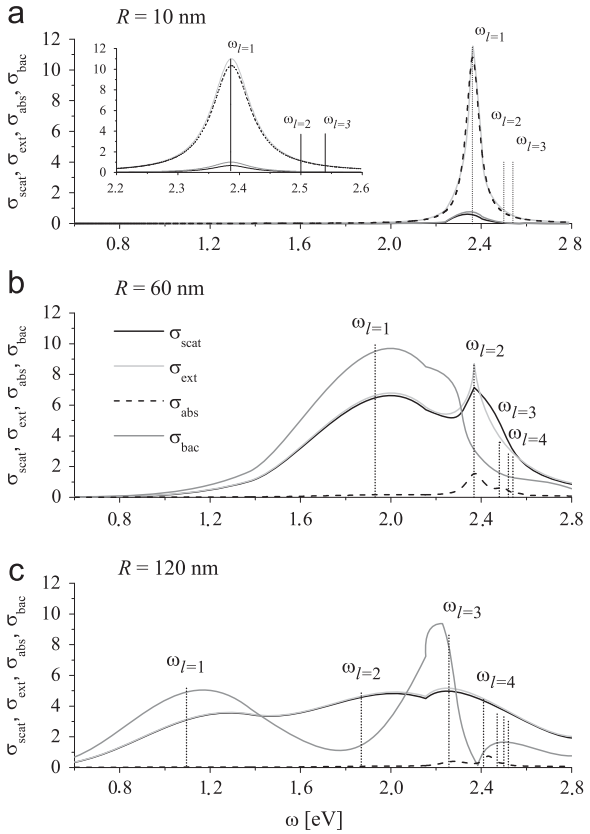

Fig. 5. The spectra of total scattering, extinction, absorbtion and backscattering differential cross-sections for gold nanospheres with radius: (a) 10 nm, (b) 60 nm and (c) 120 nm in suspension with refraction coefficient $n_{out}=1.5$. Horizontal dotted lines represent radii R_l assuring a resonance condition $\omega_{514}=\omega_l(R_l)$ as expected from solving the plasmon eigenmodes problem (see Fig. 1).

some total extinction cross-sections. In particular, the second pronounced maximum in the backscattering cross-sections (gray line in Fig. 5(b)) suffers a significant red shift with respect to the expected quadrupole plasmon position at $\omega'_{l=2}(R = 60\,\text{nm}) = 2.37\,\text{eV}$ and with respect of the corresponding maximum in the total scattering cross-section, which in turn, is shifted with respect to the maximum in the total extinction cross-section. Despite plasmon multipolar resonances are better spectrally resolved with increasing particle radius Fig. 2(a), in some measured quantities manifestation of plasmons with $l>1$ is not possible.

The effect of shifting the maxima in the scattering spectra with respect to the dipole plasmon multipolar resonances positions $\omega'_l(R)$ and smearing out of the resonances is still more pronounced for a particle as large as 120 nm in radius (Fig. 5(c)) and larger. In particular, the second maximum in the back-scattering cross-sections can not be related to the dipole plasmon manifestation at all. For given measured quantity, depending on the particle size, the result of interference of TM and TE contributions of different multipolarity influence the manner the plasmon excitation can manifest.

That illustrates the importance of looking for plasmon size characteristics within a model allowing describing plasmon excitations as the intrinsic property of a spherical nanostructure, that is detached from the quantity, which is observed.

3. Experimental determination of the size dependence of the dipole and quadrupole plasmon resonances

To check experimentally our basic expectations for surface plasmon size dependencies we need free-electron metal spheres with smoothly changeable radii. The possibility of studying the continuous change in size of optical properties of continuously growing metal sphere is not common. Such an opportunity is the most attractive feature of the light-induced sodium droplet experiment developed in our laboratory [47,48]. In addition, the spherical symmetry imposed by the surface tension of an unsupported liquid sodium droplet allows as producing almost perfect spherical scatterers. With this experimental technique we are able to determine experimentally the size dependence of the dipole and quadrupole plasmon resonances in such spheres, using the experiment geometry summarized in Section 2.3.

3.1. Scattering experiment on sodium spheres with smoothly changeable radii

Our method of sodium nanosphere production [47,48] relies on condensation of sodium spherical droplets from saturated sodium vapor. At the utilized temperatures, saturated sodium vapor consists not only of atoms, but there are also sodium dimers [48].

The successive stages of the production process are illustrated in Fig. 6.

We optically excite two-atom sodium molecules near the dissociation limit. The excited dimers become dissociated as a result of collisions with a noble gas under high pressure. Appearance of additional sodium atoms in a previously saturated atomic vapor produces supersaturation resulting in sodium droplet condensation and spontaneous growth. In our experiments, we observe the smooth change of their sizes with time up to a macroscopic droplet of about 300 nm in diameter, where the size is comparable to the wavelength of the light.

Intensities of the probe beam scattered elastically by growing droplets were measured at polarization of the light parallel and perpendicular to the observation plane (Fig. 3). The experiment was repeated for several wavelengths of the

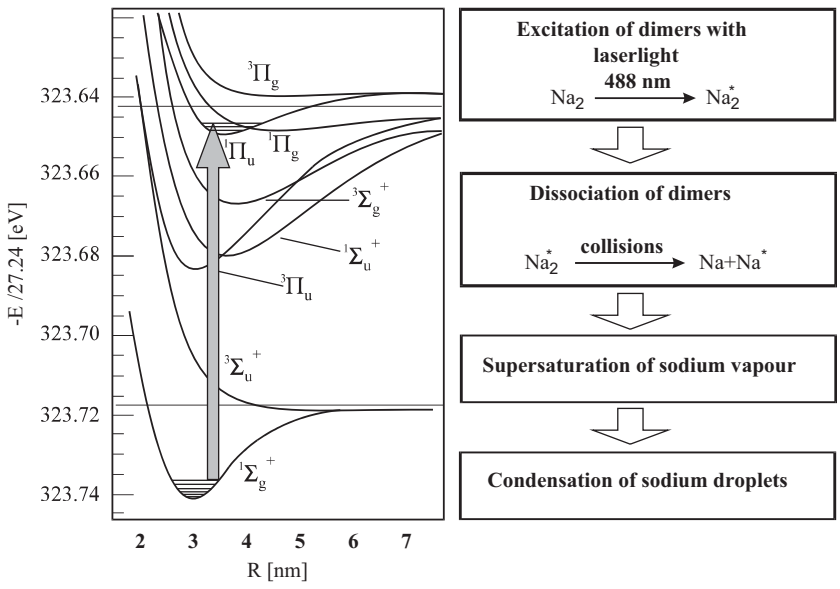

Fig. 6. Successive stages of initiating sodium droplet condensation from saturated sodium vapor with laser light.

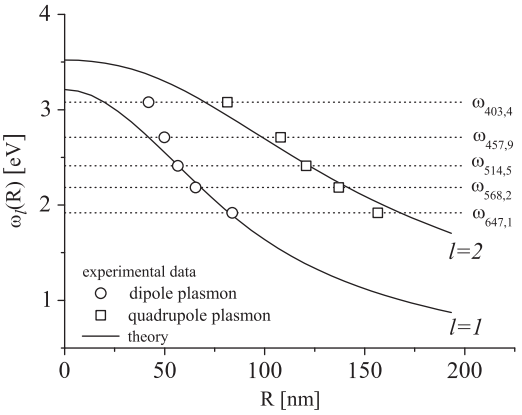

Fig. 7. Experimental dipole (circles) and quadrupole (squares) plasmon resonance positions, compared with prediction resulting from eigenvalue problem for a sodium spheres of $\omega_p = 5,6$ eV and $\gamma = 1$ eV (solid lines).

argon-ion laser light, corresponding to $\omega = 1.918$, 2.184, 2.412, 2.71, 3.079 eV. Comparison of measured intensities with calculated intensities resulting from Mie scattering theory for chosen ω (for example, for $\omega = \omega_{514}$: solid line in Fig. 4) allowed us to determine the radius and concentration of droplets at any given stage of the growth process [48]. The fitting procedure is described in more details in [48]. Using these data we are able to find the intensities scattered by the unit particle surface of a linearly polarized laser light beam in two orthogonal polarization geometries (Fig. 3) as a function of droplet radius and to identify the dipole and quadrupole plasmon resonances. We found droplet radii corresponding to the maxima of intensities: $R_{l=1}$ and $R_{l=2}$ correspondingly for different ω of the scattered wave of the laser light, as described in Section 2.3. Fig. 7 illustrates the results: circles correspond to the dipole plasmon and squares to the quadrupole plasmon positions obtained as a mean arithmetic value of the results for a group of successive scattering experiments. Solid lines represent our data resulting from eigenfrequencies consideration of sodium spheres (Section 2.2).

The error in finding the radius $R_{l=1}$ and $R_{l=2}$ for given scattering light wavelength is smaller than 10%, if determined as a standard deviation from the mean value derived from the successive scattering experiments. However, the rate of changes in concentration was not uniform during the droplet growth process. During the very first stage of droplet growth, the concentration was changing by at least three orders of magnitude. Such rapid change influenced negatively the quality of our fitting procedure, as measured by the statistical coefficient V_x defined in [48], and used as a measure of the misfit of the Mie formulae with the accepted parameters to the scattering experimental data. The parameter V_x changes approximately linearly from the value of 20% for $R = 50$ nm to 10% for $R = 120$ nm, showing much better fit for larger droplet sizes.

We also checked, that the "crossed-polarization" signals were not bigger than 10% of the studied signals and were a measure of depolarization caused by multiple reflection on the cloud of droplets and on the walls of the cell and dispersed in the directions of observation [48]. Therefore, the assumption concerning the sphericity of scatterers is well fulfilled.

The possible source of errors can be the dispersion of droplet sizes at given stage of the growth process. In [48] we abandoned the assumption concerning monodispersivity of droplet sizes in order to check whether it is possible to better reproduce the experimental scattering data with Mie theory augmented with the droplet size distribution. We assumed the dispersion of droplet sizes at a given time t and we allowed for asymmetry in the distribution of droplet sizes to distinguish between the small-size wing and the large-size wing half-widths of the size distribution. We found that the size distribution was asymmetric and broadened towards the larger droplet sizes. That can cause the overestimation of droplet sizes within the monodispersive modeling, especially for smaller size ranges (see Fig. 7).

3.2. *Experimental scattering spectra of gold and silver nanospheres of chosen radii [1–3]*

The light scattering spectra of individual gold and silver particle commercially available in various nominal sizes are measured using dark-field microscopy in [1]. Agreement with Mie scattering theory is reported to be reasonably good for the gold clusters and less satisfactory for the silver clusters. Figs. 2(a) and (c) illustrate the positions of dipole resonances (black circles) for gold and silver nanoparticles, and Fig. 2(a) illustrates the position corresponding to the quadrupole plasmon resonance (square). The emergence of the quadrupolar peak in measured spectra is reported to be expected for very large clusters where the optical field becomes nonuniform across the cluster. Based on our results presented in Fig. 2, the multipolar plasmon resonances in the largest spheres are spectrally well separated. Therefore, an observation of the quadrupole plasmon contribution to the signal in the largest spheres is more favorable. However, the distinctness of the TM quadrupole plasmon resonance contribution is smeared out due to the interference of individual multipolar contributions to the intensity in the employed observation geometry.

In [2,3] spectroscopic properties of gold particles in water are studied and particle diameter and concentration were derived from UV–vis spectra. In [3] the close agreement between the experimental and the results of Mie scattering theory

are reported. The peak positions as a function of particle size are redrawn in Fig. 2(b) (dark circles). These results are in excellent agreement with the results reported in [2] (open circles in Fig. 2 (b)). The perfect agreement is reported of the calculated extinction spectra and experimental data for particle sizes from 25 to 120 nm. As reported, for small particles this peak is damped due to the reduced mean free path of the electrons.

In [4] a study of the effect of size and shape on the spectral response of individual silver nanoparticles was presented. The maxima in the optical spectrum of many individual nanoparticles were attributed to plasmon resonances and then correlated to their size and shape using high-resolution transmission electron microscopy. The results for the dipole plasmon in spherical particles are represented as the open circles in Figs. 2(c) (in spite of the fact that the value of n_{out} is not known). The resulting size dependence of resonances position is much weaker than expected from the eigenvalue considerations and differ from the corresponding ones obtained in [1]. This can be possibly due to particle faceting or chemical reactivity of silver particles, that influence thee particle composition and change particle optical properties in comparison with the perfectly clean silver.

The experimental size dependent dipole plasmon for gold and silver spherical particles derived from peak positions of scattering spectra [1–3] are slightly red shifted in respect to the dipole plasmon size characteristics resulting from the analysis of the dispersion relation, as illustrated in Fig. 2. That is in qualitative agreement with our expectations discussed in Section 2.4 and illustrated in Fig. 5.

4. Conclusions

Surface plasmon excitations at spherical metal/dielectric interface can be described as a basic, intrinsic property of a spherical nanostructure, that can manifest in the optical response to the external electromagnetic field at discrete, characteristic, size dependent resonance frequencies $\omega'_l(R)$ specific for a given particle of radius. The resulting surface plasmon size characteristics deliver multipolar plasmon resonance frequencies and plasmon damping rate as an explicit, continuous function of particle radius and is abstracted from the quantity that can be observed in experiments relying on measuring light intensity (irradiance). Plasmon resonance takes place if the frequency ω of the incident wave approaches the plasmon resonance frequency in a sphere of radius R: $\omega = \omega'_l(R)$. The notion of surface plasmons is related to collective surface density oscillations and to the TM modes of the electromagnetic fields coupled to these oscillations, while such modes contain nonzero radial (so normal to the surface) component of the electric field.

However, the quantities which can be measured in optics (light intensities/irradiances) are inevitably composed of both TM and TE components of different polarity l. Both contributions interfere forming the complex pattern dependent on the geometry of observation and on the size of a particle in comparison with the wavelength of the light being scattered. The result of the negative interference can result in cancellation or in smearing out of the plasmon electromagnetic field contribution to the intensity of light scattered in a given direction. The resonant plasmon contribution of given l is of TM polarization only. The TE contributions of eddy currents are size dependent, but changes monotonically with particle radius R, contributing to the shift of maxima related to the resonant TM mode contribution in given measured quantity. It is why the maxima in quantities like a back scattering cross-section or a total extinction cross-sections, calculated on the base of Mie scattering theory, can differ from the multipolar plasmon resonance position, as derived from the dispersion relation for the plasmon electromagnetic fields.

The dispersion relations that we analyzed, are formally a part of Mie scattering theory and correspond to zeros of complex denominator of the ${}^{TM}B_l$ Mie coefficients (Eqs. (5)). However, Mie theory does not deal with the notion of collective surface density oscillations, neither the notion of plasmon resonances. Multipolar resonance frequencies $\omega'_l(R)$ defining the resonance condition: $\omega = \omega'_l(R)$ are not present within the formalism. No information on the radiative damping size dependence is available from such kind of study.

Multipolar plasmon resonance frequencies and plasmon damping rates expressed as a continuous function of size could be of practical use, e.g. for planning SERS experiments, allowing the optimal particle size for enhancement of the plasmon resonance electric field of frequency optimal for given molecular transition.

Acknowledgment

This work was partly supported by the Polish State Committee for Scientific Research (KBN), Grant no. 1P03B11729.

References

[1] Sönnichsen C, Franzl T, Wilk T, von Plessen G, Feldmann J. Plasmon resonances in large noble-metal clusters. New J Phys 2002;4:93.1–8.
[2] Haiss W, Thanh NTK, Aveyard J, Fernig DG. Determination of size and concentration of gold nanoparticles from UV–vis spectra. Anal Chem 2007;79:4215–21.
[3] Njoki PN, Lim I-IS, Mott D, Park H-Y, Khan B, Mishra S, et al. Size correlation of optical and spectroscopic properties for gold nanoparticles. J Phys Chem C 2007;111:14664–9.
[4] Mock JJ, Barbic M, Smith DR, Schultz DA, Schultz S. Shape effects in plasmon resonance of individual colloidal silver nanoparticles. J Chem Phys 2002;116:6755–9.

[5] Daniel M-C, Astruc D. Gold nanoparticles: assembly, supramolecular chemistry, quantum-size-related properties, and applications toward biology, catalysis, and nanotechnology. Chem Rev 2004;104(1):293–346.
[6] Quinten M, Leitner A, Krenn J, Aussenegg F. Electromagnetic energy transport via linear chains of silver nanoparticles. Opt Lett 1998;23(17):1331–3.
[7] Maier SA, Brongersma ML, Kik PG, Atwater HA. Observation of near-field coupling in metal nanoparticle chains using far-field polarization spectroscopy. Phys Rev B 2002;65(19):193408.1–4.
[8] Dickson RM, Lyon LA. Unidirectional plasmon propagation in metallic nanowires. J Phys Chem B 2000;104(26):6095–8.
[9] Brongersma ML, Hartman JW, Atwater HA. Electromagnetic energy transfer and switching in nanoparticle chain arrays below the diffraction limit. Phys Rev B 2000;62:R16356–9.
[10] Krenn JR, Lamprecht B, Ditlbacher H, Schider G, Salerno M, Leitner A, et al. Non-diffraction-limited light transport by gold nanowires. Europhys Lett 2002;60(5):663–9.
[11] Kneipp K, Kneipp H, Kartha VB, Manoharan R, Deinum G, Itzkan I, et al. Detection and identification of a single DNA base molecule using surface-enhanced Raman scattering (SERS). Phys Rev E 1988;57(6):R6281–4.
[12] Faulds K, Smith WE, Graham D. Evaluation of surface-enhanced resonance raman scattering for quantitative DNA analysis. Anal Chem 2004;76(2):412–7.
[13] Efrima S, Bronk BV. Silver colloids impregnating or coating bacteria. J Phys Chem B 1998;102(31):5947–50.
[14] Kneipp K, Wang Y, Dasari RR, Feld MS. Near-infrared surface-enhanced Raman scattering (NIR-SERS) of neurotransmitters in colloidal silver solutions. Spectrochim Acta A 1995;51A(3):481–7.
[15] Schultz S, Smith DR, Mock JJ, Schultz DA. Single-target molecule detection with nonbleaching multicolor optical immunolabels. PNAS 2000;97(3):996–1001.
[16] Schultz S, Mock J, Smith DR, Schultz DA. Nanoparticle based biological assays. J Clin Ligand Assay 1999;22:214–6.
[17] Yguerabide J, Yguerabide EE. Anal Biochem 1998;262:157–76.
[18] Raether H. In: Surface plasmons on smooth and rough surfaces and on gratings. Springer tracts in modern physics, vol. 111. Berlin, Heidelberg: Springer; 1988.
[19] Cottam MG, Tilley DR. Introduction to surface and superlattice excitations. New York: Cambridge University Press; 1989.
[20] Fuchs R, Halevi P. Basic concepts and formalism of spatial dispersion. In: Spatial dispertion in solids and plasmas. Amsterdam: North-Holland; 1992.
[21] Rupin R. Electromagnetic surface modes. Chichester: Wiley; 1982.
[22] Jana NR, Gearheart L, Murphy CJ. Seed-mediated growth approach for shape-controlled synthesis of spheroidal and rod-like gold nanoparticles using a surfactant template. Adv Mater 2001;13(18):1389–93.
[23] Orendorff CJ, Murphy CJ. Quantitation of metal content in the silver-assisted growth of gold nanorods. J Phys Chem B 2006;110(9):3990–4.
[24] Liao H, Hafner JH. Gold nanorod bioconjugates. Chem Mater 2005;17(18):4636–41.
[25] Schider G, Krenn JR, Hohenau A, Ditlbacher H, Leitner A, Aussenegg FR, et al. Plasmon dispersion relation of Au and Ag nanowires. Phys Rev B 2003;68:155427.1–4.
[26] Schaich WL, Schider G, Krenn JR, Leitner A, Aussenegg FR, Puscasu I, et al. Optical resonances in periodic surface arrays of metallic patches. Appl Opt 2003;42(28):5714–21.
[27] Payne EK, Shuford KL, Park S, Schatz GC, Mirkin CA. Multipole plasmon resonances in gold nanorods. J Phys Chem 2006;110(5):2150–4.
[28] Khlebtsov BN, Melnikov A, Khlebtsov NG. On the extinction multipole plasmons in gold nanorods. J Quant Spectrosc Radiat Transfer 2007;107(2):306–14.
[29] Millstone JE, Park S, Shuford KL, Qin L, Schatz GC, Mirkin CA. Observation of a quadrupole plasmon mode for a colloidal solution of gold nanoprisms. J Am Chem Soc 2005;127(15):5312–3.
[30] Derkachova A, Kolwas K. Size dependence of multipolar plasmon resonance frequencies and damping rates in simple metal spherical nanoparticles. Eur J Phys ST 2007;144:93–9.
[31] Kolwas K, Derkachova A, Demianiuk S. The smallest free-electron sphere sustaining multipolar surface plasmon oscillation. Comput Mater Sci 2006;35:337–41.
[32] Kolwas K, Demianiuk S, Kolwas M. Optical excitation of radius-dependent plasmon resonances in large metal clusters. J Phys B 1996;29:4761–70.
[33] Kolwas K, Demianiuk S, Kolwas M. Dipole and quadrupole plasmon resonances in large sodium clusters observed in scattered light. J Chem Phys 1997;106:8436–41.
[34] Faraday M. Experimental relations of gold and other metals to light. Philos Trans R Soc London 1857;147:145–81.
[35] Mie G. Beiträge zur Optik trüber Medien, speziell kolloidaler Metallösungen. Ann Phys 1908;25:376–445.
[36] ⟨http://people.ee.duke.edu/~drsmith/plasmon_nanostructures.htm⟩.
[37] Mishchenko MI, Travis LD, Lacis AA. Scattering, absorption and emission of light by small particles. Cambridge: Cambridge University Press; 2002.
[38] Born M, Wolf E. Principles of optics. Oxford: Pergamon; 1975.
[39] Bohren CF, Huffmann DR. Absorption and scattering of light by small particles. New York: Wiley; 1983.
[40] Stratton JA. Electromagnetic theory, international series in physics. New York: McGraw-Hill; 1941.
[41] Raether H. In: Excitation of plasmons and interband transitions by electrons. Springer tracts in modern physics, vol. 88. Berlin, Heidelberg, New York: Springer; 1980.
[42] Kreibig U, Vollmer M. Optical properties of metal clusters. Springer series in material science, vol. 25. Berlin: Springer; 1995.
[43] de Heer WA. The physics of simple metal clusters: experimental aspects and simple models. Rev Mod Phys 1993;65(3):611–76.
[44] Forstmann F, Gerhardts RR. Metal optics near the plasma frequency. Springer tracts in modern physics, vol. 109. Berlin, Heidelberg: Springer; 1986.
[45] Pinchuk A, Kreibig U, Hilger A. Optical properties of metallic nanoparticles: influence of interface effects and interband transitions. Surf Sci 2004;557(1–3):269–80.
[46] Johnson PB, Christy RW. Optical constants of the noble metals. Phys Rev B 1972;6:4370–9.
[47] Kolwas M, Kolwas K, Jakubczyk D. Sodium clusters produced by laser light. Appl Phys B 1995;60:S173–81.
[48] Demianiuk S, Kolwas K. Dynamics of spontaneous growth of light-induced sodium droplets from the vapour phase. J Phys B 2001;34:1651–71.